

Effects of Matrix-to-analyte Ratio and Laser Energy on Peptides Ion Signals

This article has been downloaded from IOPscience. Please scroll down to see the full text article.

2006 Chin. J. Chem. Phys. 19 207

(<http://iopscience.iop.org/1003-7713/19/3/007>)

View [the table of contents for this issue](#), or go to the [journal homepage](#) for more

Download details:

IP Address: 61.190.88.144

The article was downloaded on 16/11/2012 at 02:24

Please note that [terms and conditions apply](#).

ARTICLE

Effects of Matrix-to-analyte Ratio and Laser Energy on Peptides Ion Signals

Liu-zhu Zhou^{a,b}, Yuan Zhu^a, Xiao-yong Guo^a, Wen-wu Zhao^a, Hai-yang Zheng^a, Xue-jun Gu^a,
Li Fang^{a*}, Wei-jun Zhang^a

a. Lab of Environmental Spectroscopy, Anhui Institute of Optics and Fine Mechanics, Chinese Academy of Sciences, Hefei 230031, China; b. Qufu Normal University, Qufu 273165, China

(Dated: Received on April 4, 2005; Accepted on August 22, 2005)

A method of aerosol introduction for matrix-assisted laser desorption/ionization (MALDI) is described. The aerosol particles containing matrix and analyte enter directly into the aerosol time-of-flight mass spectrometer (ATOFMS) at atmospheric pressure. The scattered light signals from the aerosol particles are collected by a photomultiplier tube (PMT) and are passed on to an external electronic timing circuit, which determines particle size and is used to trigger a 266 nm pulsed Nd:YAG laser. The aerosol MALDI mass spectra and aerodynamic diameter of single particles can be obtained in real-time. Compared with other methods of liquid sample introduction, this method realizes detection of single particles and, more importantly, the sample consumption is lower. The effects of matrix-to-analyte ratio and laser pulse energy on analyte ion yield are examined. The optimal matrix-to-analyte ratio and laser energy are 50-110:1 and 200-400 μ J respectively.

Key words: ATOFMS, MALDI, Matrix, Peptides

I. INTRODUCTION

The matrix assisted laser desorption/ionization (MALDI) technique [1], developed in 1987, has matured into a valuable tool in the biosciences for obtaining both accurate mass determinations and primary sequence information. In most cases, molecular ions are produced with little or no fragmentation. Although the MALDI technique is well established, there is still a great deal of room for improvement, particularly in the area of sample introduction. While advances have been made in automated sample preparation and analysis, a typical MALDI sample preparation involves manually depositing a solution of matrix and analyte on a sample probe and waiting for solvent evaporation before insertion of the sample probe into the mass spectrometer.

There have been several attempts to develop direct liquid introduction methods. Such a method, one that uses aerosols for direct liquid introduction, has already been reported. The aerosol MALDI interface is an extension of these previous aerosol liquid introduction methods [2]. In the aerosol MALDI method, a solution of matrix and analyte is sprayed into the mass spectrometer with a liquid flow rate of up to 0.5-1 mL/min. A high-speed pumping system and a heated drying tube are used to remove solvent and carrier gas. The dried aerosol particles are irradiated with pulsed UV laser radiation to form protonated analyte ions. A main drawback of aerosol MALDI is higher sample consumption.

The analyte, gramicidin-s, is consumed at 1.48 mg/min or more. Current work on the aerosol MALDI instrument is focused on implementing a single particle interface. If single particles can be delivered to the ion source and be ionized with a synchronized pulsed laser, sample consumption will be reduced by many orders of magnitude. Recently, we developed an aerosol time-of-flight mass spectrometer (ATOFMS). Aerosol particles containing matrix and analyte are directly injected into ATOFMS at atmospheric pressure. The aerodynamic diameter and MALDI mass spectra for each particle are obtained simultaneously.

Our current work on aerosol MALDI is focused on developing a better understanding of the experimental parameters that influence the ionization process. The experimental parameters include sample preparation, matrix, laser intensity and molar ratio of the matrix-to-analyte *et al.* In this work, we focus on two parameters: (i) matrix-to-analyte ratio and (ii) laser pulse energy.

II. EXPERIMENTAL SECTION

The ATOFMS apparatus has been described elsewhere in detail [3] and will only be outlined here. Figure 1 shows a schematic diagram of the experimental configuration. The aerosol particles first enter an inlet of ATOFMS, which consists of a capillary (3.5 mm i.d \times 110 mm) and a nozzle with diameter 0.3 mm. The inlet region draws in air and entrained particles at a rate of 0.8 L/min. The pressure at the exit region of nozzle is maintained at \sim 260 Pa. After supersonic expansion through the nozzle, the aerosol beam passes through two stages of differential pumping regions sep-

* Author to whom correspondence should be addressed. E-mail: fangli@aiofm.ac.cn, Tel: 0551-5591152

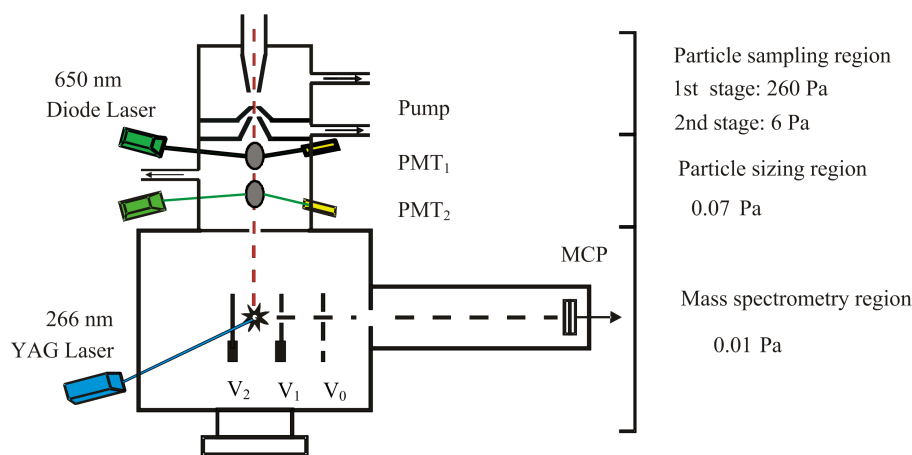


FIG. 1 Experimental configuration of the ATOFMS instrument.

arated by two skimmers with diameters of 0.5 mm. The two regions operate at pressures of 6 and 0.07 Pa. The skimmers also serve to collimate the particle stream into a narrow beam.

Once in the particle sizing region, each particle encounters two continuous wave lasers produced by 50 mW diode lasers (Science & Technology Development Co., Ltd. Xi'an of China) operating at 650 nm. The scattered light from the particle is collected by a photomultiplier tube (PMT, BinSong corporation, Beijing of China). The particle then travels 70 mm where it encounters a second diode laser. Scattered light from this laser is collected by a second PMT detector. The electronic signals from the two PMTs are passed on to an external timing circuit. The velocity of the particle can be determined by the distance between the two scattering lasers and the delay between the two scattering pulses. The velocity and size of the particle are directly related, and upon performing the appropriate calibration studies, this relationship will be used for the determination of single particle sizes. The time delay between the two scattering pulses is also used to synchronize the firing of a 266 nm pulse from a frequency-quadrupled Nd:YAG laser.

The Nd:YAG laser was used for both the desorption and ionization processes. The pulse width is 10 ns, and the diameter of UV laser spot was approximately 500 μm . A power density of 3×10^6 to 2×10^7 W/cm² was selected. The pressure in the ionization region was approximately 10^{-5} Pa. The voltage was +2.5 kV on the repulsion electrode and +2 kV on the acceleration electrode. The resulting ions were accelerated in the ion source toward the microchannel plates (MCP, Institute of Electronics, Chinese Academy of Sciences). The signals from MCP were sent to a personal computer via a 50 Ω coaxial cable, the data was then further processed by a data system developed in-house. The instrument, therefore, provided the aerodynamic size and a chemical

mass spectrum for single particles.

III. RESULTS AND DISCUSSION

Sample solutions were made from matrix and analyte dissolved in methanol, while trifluoroacetic acid (Chemicals reagents corporation, Shanghai of China) was added to the solutions at 0.4 volume percent as a proton source. The matrix compound 2,5-dihydroxybenzoic acid (DHB, Sigma, G-5254) and the analyte six-peptide (Sangon, P00992, C₂₆H₃₉N₉O₁₁, MW=653) were used without further purification. The solution contained 0.4 g/L analyte, and the matrix concentrations were varied. The molar ratio of matrix to analyte varied from 12:1 to 500:1. The aerosol particles were generated using nitrogen carrier gas at a flow rate of 5 L/min in a Devilbiss 40[#] nebulizer (D40), and were collected by a 10 L glass bottle equipped with an inlet and a outlet in order to maintain balance of atmospheric pressure. The inlet was connected to a filter (Balston DFU, USA), and the outlet was directed into the inlet of ATOFMS with a soft tube.

When the matrix-to-analyte ratio varies, the particle size also changes. The size distribution of an aerosol particle is independently monitored with an aerodynamic particle sizer spectrometer (model 3321; TSI, St. Paul, MN). Particles used in these experiments range in size from 0.4 μm to 3 μm . Figure 2 shows the results from mean aerodynamic diameter of the aerosol measured during an experiment with TSI 3321. The mean particle size first increases rapidly and then levels off when the matrix-to-analyte ratio exceeds 250:1. At which point, the solution may reach saturation. The results indicate that the optimal matrix-to-analyte ratio should be less than 250:1.

Figure 3 shows a MALDI mass spectrum of six-peptide in DHB. The mass spectrum is calibrated using

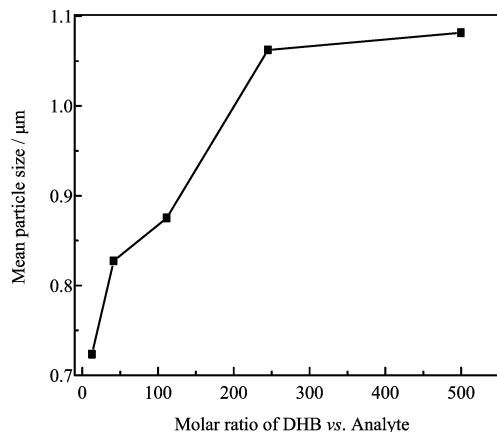


FIG. 2 The plot of the mean particle size as a function of matrix-to-analyte ratio.

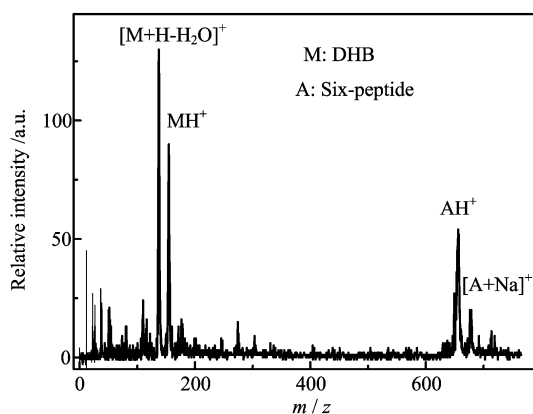


FIG. 3 MALDI mass spectra of six-peptide in DHB. DHB/six-peptide molar ratio, 110:1

ion generated from DOP (Diocetyl Phthalate, Chemicals Factory of Xudong, Beijing, China). The particle diameter is $1.2 \mu\text{m}$, the molar ratio of DHB to six-peptide is 110:1 and the laser pulse energy is $300 \mu\text{J}$. Figure 3 shows typical characteristics of an aerosol MALDI mass spectrum. The protonated analyte molecular ion, denoted AH^+ , is observed at approximate m/z 654. The sodium adduct ion, $[\text{A}+\text{Na}]^+$, is also present. The appearance of Na^+ indicates salt impurity, which may originate from the matrix, the analyte, solvents, glassware or from the surface of the sample carrier [4]. Knochenmuss and Zenobi postulated that the alkali adduct ion is generated by gas-phase cation transfer [5,6]. In the low mass region, the protonated matrix molecular ion, MH^+ , and the matrix fragment ion, $[\text{M}+\text{H}-\text{H}_2\text{O}]^+$, are responsible for the main ion peaks.

Figure 4 contains plots of the integrated MH^+ and AH^+ peak area as a function of the matrix-to-analyte ratio. The laser desorption/ionization pulse energy is $300 \mu\text{J}$. In Fig.4 each datum is the average of 10 single particle spectra, and the error bars represent the

standard deviation of the mean. The aerodynamic diameters ranged from $0.7 \mu\text{m}$ to $1.5 \mu\text{m}$. In our previous studies, signal intensity was relatively invariant with respect to particle size in the diameter range. Note, the AH^+ ion signal rises very quickly at matrix-to-analyte ratios less than 110:1, and decreases very slowly at matrix-to-analyte ratios larger than 110:1, while the MH^+ ion signal is relatively invariant. These results show the concentration of matrix influence on protonated analyte ion, so the optimum matrix-to-analyte ratios should be in the range of 50-110:1, which is lower than surface MALDI [7]. In surface MALDI, the optimum matrix-to-analyte ratio is typically 10^2 - 10^4 :1. The differences between surface MALDI and aerosol MALDI are related to the rate of crystal formation. Fast crystallization forces the matrix and analyte into contact and favors a low matrix-to-analyte ratios. In a previous aerosol MALDI, Murray detected matrix-to-analyte ratios in the range of 30-100:1, where the concentration of the matrix is held constant, and the concentration of the analyte is varied [8].

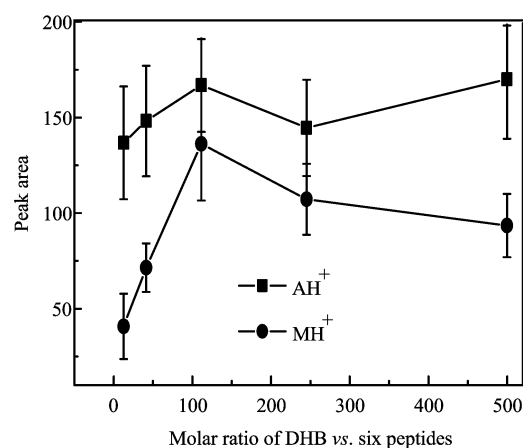


FIG. 4 The plot of the MH^+ and AH^+ peak area as a function of matrix-to-analyte mole ratio.

Figure 5 contains mass spectra of six-peptide at different laser energies (100, 200, and $400 \mu\text{J}$). The matrix-to-analyte ratio used was 100:1. These spectra are similar to Fig.3. Between 100 and $200 \mu\text{J}$, the signal intensity rises very quickly and no protonated analyte ions are observed below $100 \mu\text{J}$ pulse energy. This corresponds to an apparent threshold for ion production of $0.1 \text{ J}/\text{cm}^2$, which is significantly higher than that in conventional MALDI [9] but comparable to a previous aerosol MALDI experiments [10,11].

Above the threshold, the signal intensity has a relatively weak dependence on laser energy, but the fragment ion signals increase in the low mass regions. Additionally, protonated clusters of DHB, specifically $[2\text{M}+\text{H}-2\text{H}_2\text{O}]^+$ [12], are also observed. So the optimum laser pulse energy is estimated in the range of 200-400 μJ .

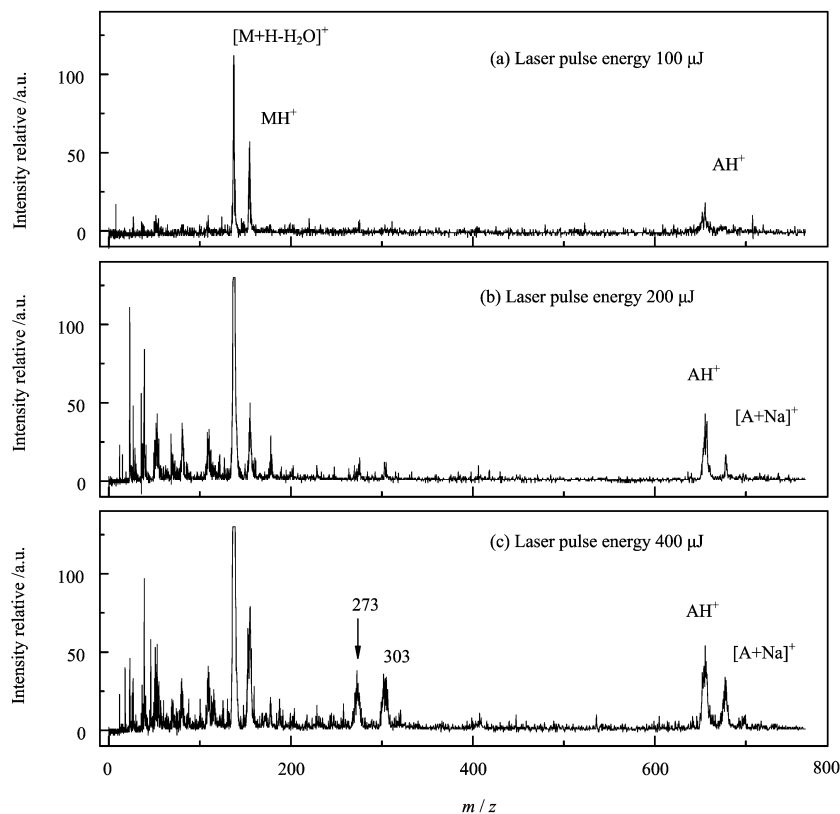


FIG. 5 MALDI mass spectra of six peptides at different laser energies.

IV. CONCLUSIONS

In aerosol MALDI mass spectra, there are many experimental parameters that influence the ionization process. The results show that the protonated analyte ion signal intensity can be systematically varied by selecting different experimental parameters. We have discussed the molar ratio of matrix to analyte and laser pulse intensity influence on protonated analyte ion signal intensity in order to correctly select the parameters. When the laser pulse energy and the concentration of analyte are held constant, the signal intensity is relatively invariant with the molar ratio of matrix to analyte. When molar ratio of matrix to analyte is held constant, above the threshold, the signal intensity first increases and then levels off.

The advantages of aerosol MALDI for the detection of single particles are: (i) the ability to simultaneously obtain the size and chemical composition of the single particle; (ii) lower sample consumption. The aerosol particles can be generated continually by D40 with 3 mL solution containing analyte and matrix. This method of aerosol introduction can lead to a highly efficient aerosol MALDI source.

- [1] M. Karas, D. Bachmann, U. Bahr, *et al.* *Int. J. Mass Spectrom. Ion Process.* **78**, 53 (1987).
- [2] K. K. Murray and D. H. Russell, *Anal. Chem.* **65**, 2534 (1993).
- [3] Z. H. Xia, L. Fang, H. Y. Zheng, *et al.* *Chin. J. Anal. Chem.* **32**, 973 (2004).
- [4] J. Zhang and R. Zenobi, *J. Mass Spectrom.* **3**, 808 (2004).
- [5] R. Zenobi and R. Knochenmuss, *Mass Spectrom. Rev.* **17**, 337 (1998).
- [6] R. Knochenmuss and R. Zenobi, *Chem. Rev.* **103**, 441 (2003).
- [7] M. Karas and F. Hillenkamp, *Anal. Chem.* **60**, 2299 (1988).
- [8] M. D. Beeson, K. K. Murray and D. H. Russell, *Anal. Chem.* **67**, 1981 (1995).
- [9] K. Dreisewerd, M. Schurenberg, M. Karas, *et al.* *Int. J. Mass Spectrom. Ion Processes* **141**, 127 (1995).
- [10] B. A. Mansoori, M. V. Johnston and A. S. Wexler, *Anal. Chem.* **66**, 3681 (1994).
- [11] B. A. Mansoori and M. V. Johnston, *Anal. Chem.* **68**, 3595 (1996).
- [12] X. J. Gu, L. Z. Zhou, Z. Y. Wang, *et al.* *Chin. J. Chem. Phys.* **18**, 308 (2005).